



ELSEVIER

Contents lists available at ScienceDirect

Data in brief

journal homepage: www.elsevier.com/locate/dib

Data Article

Prediction of functional consequences of the five newly discovered G6PD variations in Taiwan



Yen-Hui Chiu ^{a, b, 1}, Yu-Ning Liu ^{a, 1}, Hsiao-Jan Chen ^c,
 Ying-Chen Chang ^{d, 2}, Shu-Min Kao ^c, Mei-Ying Liu ^c,
 Ying-Yen Weng ^d, Kwang-Jen Hsiao ^{a, e, **, 1}, Tze-Tze Liu ^{a, d, *}

^a Department of Education and Research, Taipei City Hospital, Taipei, Taiwan^b Department of Biotechnology and Pharmaceutical Technology, Yuanpei University of Medical Technology, Hsinchu, Taiwan^c Neonatal Screening Center, The Chinese Foundation of Health, Taipei, Taiwan^d Cancer Progression Research Center, National Yang-Ming University, Taipei, Taiwan^e Preventive Medicine Foundation, Taipei, Taiwan

ARTICLE INFO

Article history:

Received 25 April 2019

Received in revised form 28 May 2019

Accepted 3 June 2019

Available online 11 June 2019

Keywords:

G6PD deficiency

Mutation analysis

In silico analysis

Structural predication

ABSTRACT

Glucose-6-phosphate dehydrogenase deficiency (G6PD deficiency; OMIM #300908) is the most common inborn error disorders worldwide. While the G6PD is the key enzyme of removing oxidative stress in erythrocytes, the early diagnosis is utmost vital to prevent chronic and drug-, food- or infection-induced hemolytic anemia. The characterization of the mutations is also important for the subsequent genetic counseling, especially for female carrier with ambiguous enzyme activities and males with mild mutations. While multiplex SNaPshot assay and Sanger sequencing were performed on 500 G6PD deficient males, five newly discovered variations, namely c.187G > A (p.E63K), c.585G > C (p.Q195H), c.586A > T (p.I196F), c.743G > A (p.G248D), and c.1330G > A (p.V444I) were detected in the other six patients. These variants were previously named as the Pingtung, Tainan, Changhua, Chiayi, and Tainan-2 variants, respectively. The *in silico* analysis, as well as the prediction of the structure of the resultant mutant G6PD

* Corresponding author. Cancer Progression Research Center, National Yang-Ming University, No.155, Sec. 2, Li-Nong Street, Taipei 11221, Taiwan.

** Corresponding author. Preventive Medicine Foundation, Taipei P.O. Box 26-553, Taipei 10699, Taiwan

E-mail addresses: hsiao@pmf.tw (K.-J. Hsiao), ttliu@ym.edu.tw, tze@pmf.tw (T.-T. Liu).

¹ The three authors contributed equally to this work.

² Current position: Excelsior Pharmatech Labs, Taipei, Taiwan.

protein indicated that these five newly discovered variants might be disease causing mutations.

© 2019 The Authors. Published by Elsevier Inc. This is an open access article under the CC BY license (<http://creativecommons.org/licenses/by/4.0/>).

Specifications table

Subject area	Genetics, Genomics and Molecular Biology
More specific subject area	Inborn errors of metabolism
Type of data	Tables, Figures
How data was acquired	DNA sequencing using 3730xl Genetic Analyzer (Thermo Fisher Scientific, Waltham, MA, USA), mutation severity prediction softwares, structural effect prediction software
Data format	Analyzed
Experimental factors	DNA extracted from dried blood spot used in newborn screening
Experimental features	Bioinformatic tools
Data source location	Taiwan
Data accessibility	Provided within this article
Related research article	Chiu YH, Chen HJ, Chang YC, Liu YN, Kao SM, Liu MY, Weng YY, Hsiao KJ, Liu TT. Applying a multiplexed primer extension method on dried blood spots increased the detection of carriers at risk of glucose-6-phosphate dehydrogenase deficiency in newborn screening program. Clin. Chim. Acta 495 (2019) 271–277. https://doi.org/10.1016/j.cca.2019.04.074 [1].

Value of the Data

- This study extends the *G6PD* mutation spectrum.
- The three-dimensional structure illustrates the importance of the amino acid residues related to the function of the *G6PD* protein.
- The *in silico* analysis served as a tool in determining the functional consequence of the mutations, making it potentially valuable for primary care as well as research processes.

1. Data

This dataset presented the *in silico* and structural analysis of the five newly discovered variations, namely c.187G > A (p.E63K), c.585G > C (p.Q195H), c.586A > T (p.I196F), c.743G > A (p.G248D), and c.1330G > A (p.V444I) (Fig. 1), detected in the six Taiwanese *G6PD* deficient patients using Sanger Sequencing (Table 1).

The comparison sequence of these variants in *G6PD* protein of different species [2], including *Homo sapiens*, *Mus musculus*, *Danio rerio* (zebrafish), *Drosophila melanogaster* (fruit fly), and *Caenorhabditis elegans* were presented in Fig. 2. The *in silico* analysis using SIFT [3], PolyPhen-2 [3], Mutation Taster [4] and Slicing Finder [5] softwares, as well as the conservation between species and allele frequency in Taiwanese population [6] were summarized in Table 2. Furthermore, the amino acid alterations were presented in the functional domains [7] (Fig. 3) and in partial 3D model of *G6PD* [8] (Fig. 4). The structure of the resultant mutant *G6PD* protein were analyzed by HOPE, Have yOur Protein Explained [9] (Table 3).

2. Experimental design, materials and methods

2.1. Mutation identification: sanger sequencing

In 500 *G6PD*-deficient male newborns detected by *G6PD* enzyme activity assay [10], nine of which do not carry any of the 21 common mutations described in Taiwan and Southeast Asia using multiplex

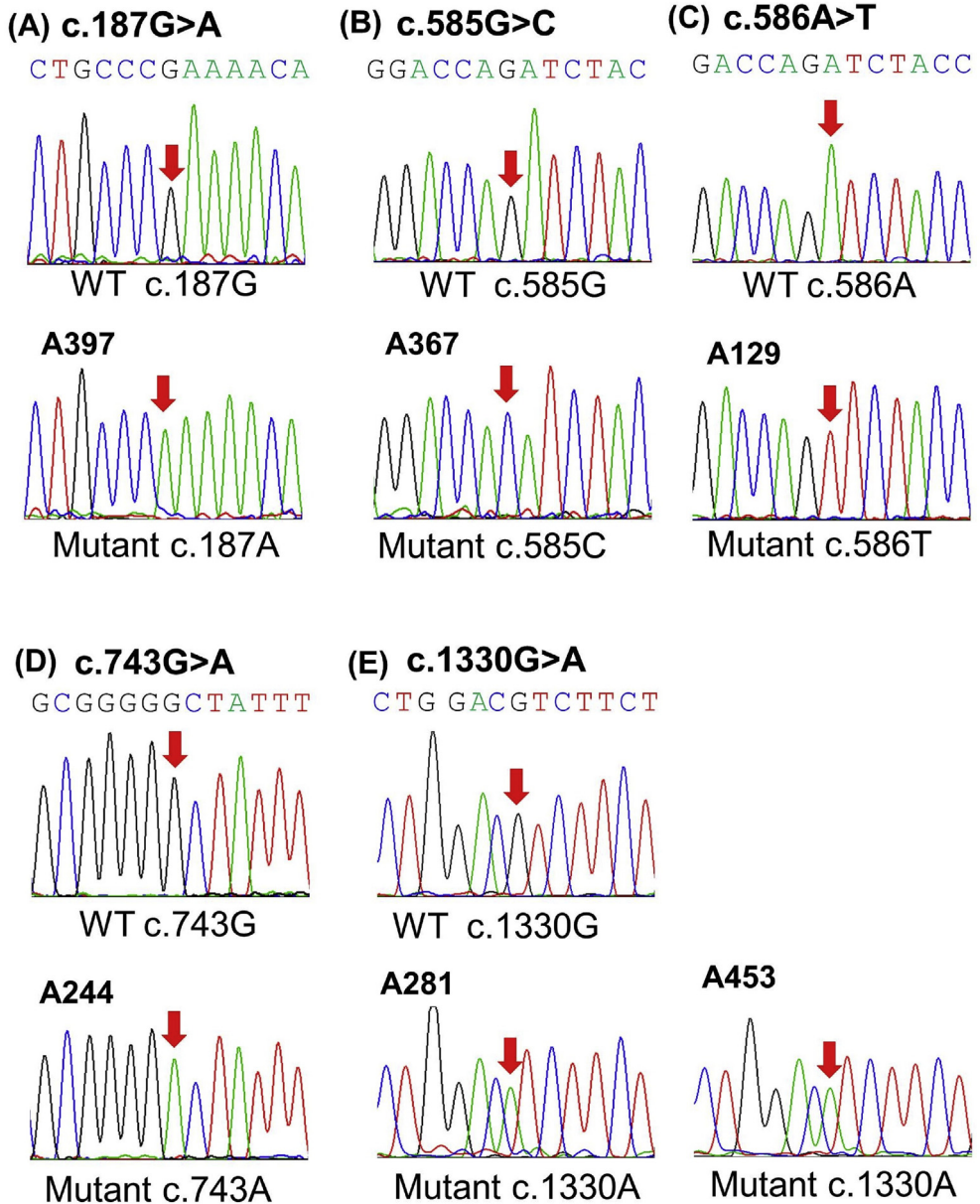


Fig. 1. Detection of five new *G6PD* variations by Sanger sequencing. *G6PD* gene sequence showed the wild type sequence with variants of different individuals. (A) c.187G > A in patient A397, (B) c.585G > C in patient A367, (C) c.586A > T in patient A 129, (D) c.743G > A in patient A244 and (E) c.1330G > A in patients A281 and A453. The red arrows showed substitution in a hemizygous state in the missense mutations observed.

SNAPshot assay [1]. Their dried blood spots used in newborn screening were subsequently subjected to mutational analysis by sequencing. The whole coding exons and exon-intron boundary sequences of

Table 1

G6PD activity in newborn screening and following referral for patients carrying newly discovered G6PD variations.

Patient Number	A129	A244	A281	A367	A397	A453
Sex	Male	Male	Male	Male	Male	Male
Place of Birth	Changhua	Chiayi	Tainan	Tainan	Pingtung	Tainan
Age at newborn screening (day)	2	2	2	2	3	3
G6PD activity in newborn screening (U/gHb) ^a	0.2	5.5	5.3	1.7	5.7	5.1
Age when confirmed (day)	34	9	22	15	14	11
Confirmed G6PD activity (U/gHb) ^b	0.1	6.1	5.5	0.2	8.6	6.5
Variation found	c.586A > T	c.743G > A	c.1330G > A	c.585G > C	c.187G > A	c.1330G > A

^a Clinical referral was recommended for those enzyme activity ≤ 6.0 U/gHb.

^b The confirmed diagnosis was performed through a quantitative enzyme activity assay by using fresh whole blood. G6PD-deficiency would be suggested for those with G6PD activity ≤ 10.0 U/gHb.

G6PD gene were amplified and analyzed by forward and reverse Sanger sequencing. Putative mutations were confirmed by sequencing of an independent PCR product. The study protocol was reviewed and approved by the Institutional Review Board of Taipei City Hospital, Taiwan.

2.2. Sequence alignments between species

Conservation of the peptide sequence around the affected residues was assessed by alignment of orthologous and human G6PD sequences with ClustalW2, [2].

2.3. Severity prediction and allele frequency in population

Different online algorithms were used to predict the functional consequences of the five variants. The *in silico* analyses were performed using the SIFT [3], PolyPhen-2 [3], MutationTaster2 [4], and Human Splicing Finder [5] programs. Furthermore, the allele frequency of the alterations in Taiwanese population was listed as provided in Taiwan Biobank [6].

2.4. Distribution of mutations along the coding region and protein sequence

Distribution of alterations was highlighted in the coding region and the functional domains [7]. The A at the ATG translational initiation codon was numbered as 1 in reference accession number NM_001042351. The amino acid numbers were counted from the N-terminal Met of human G6PD protein.

2.5. 3D structure model of wide type G6PD protein

The 3D structure of G6PD variations observed in this study were presented based on the X-ray crystal structure available at the Protein Data Bank from human G6PD protein (PDB code 1QKI) [8].

2.6. Prediction of structural effects of variations

When protein structure is important to predict the effects of variants [11], effect of mutations over G6PD protein structure was determined using HOPE (Have yOur Protein Explained) software [9].

<i>Homo sapiens</i>	001	MAEQVALSRTQVCGILREELFQGDAFHQSDTHIFIIMGASGLAKKKIYPTIWWLFRDGL	060
<i>Mus musculus</i>	001	MAEQVALSRTQVCGILREELYQGDAFHQADTHIFIIMGASGLAKKKIYPTIWWLFRDGL	060
<i>Danio rerio</i>	015	-----LSRSEVFGQLRKELHDDTAFHQSDVHIFIIMGASGLAKKKIYPTLWWLFRDGL	068
<i>D. melanogaster</i>	020	-----SPTMVC-----EGTHFDGKIPIHTFVIFGASGLAKKKIYPTLWWLYRDDL	064
<i>C. elegans</i>	034	-----FGASGLAKKKIYPTLWWLFRDNL	062
p.E63K			
<i>Homo sapiens</i>	061	LPENTFIVGYARSRLTVADIRKQSEPFKATPEEKLKLEDFFARNYSVAGYDDAASYQR	120
<i>Mus musculus</i>	061	LPEDTFIVGYARSRLTVDDIRKQSEPFKATPEERPKLEEFFARNYSVAGYDDAASYKH	120
<i>Danio rerio</i>	069	LPBQTYFVGFARSDLTVDAIRIACMPYMKVVDNEAERLAAFFSRNSYISGKYVEESSFS	128
<i>D. melanogaster</i>	065	LPKPTKFCGYARSMLTVDSIKEQCLPYMKVQPHEQKKEEFWALNEYVSGRYDGRGTGFEL	124
<i>C. elegans</i>	063	LPVNIKIFIGYARSLTVFKLRESFEKNCKVRENEKCAFDDFIKCKSYVQGYDTSSEGFQR	122
<i>Homo sapiens</i>	121	LNSHMNALHLGSQ---ANRLFYLALPPTVYEAVTKNIHESCMSQ-IGWNRIIVEKPFGRDLQSS	180
<i>Mus musculus</i>	121	LNSHMNALHQGMQ---ANRLFYLALPPTVYEAVTKNIQETCMSQ-TGWNRIIVEKPFGRDLQSS	180
<i>Danio rerio</i>	129	LNTHLLSLPGGAE---ANRLFYLALPPSVYHDVTKNIKHQCMST-KGWNRVYIEKPFGRDLQSS	188
<i>D. melanogaster</i>	125	LNQLEIMENKKNK---ANRLFYLALPPSVFEEVTVNIKIQICMSV-TGWNRVYIEKPFGRDDASS	184
<i>C. elegans</i>	123	LQSSIDDFQKESNNQAVNRLYYLALPPSVFNVVSTELKKNCMDHGDSWTRVYIEKPFGRDLQSS	186
p.Q195H p.I196F			
<i>Homo sapiens</i>	181	DRLSNHISLRFREDQTYRIDHYLGKEMVQNLMLVLRFANRIFGPIWNRDNIACVILTFKEP	240
<i>Mus musculus</i>	181	NQLSNHISLRFREDQTYRIDHYLGKEMVQNLMLVLRFANRIFGPIWNRDNIACVILTFKEP	240
<i>Danio rerio</i>	189	EELSSHLSLRFTEBQTYRIDHYLGKEMVQNLMLVLRFGNRIFGPIWNRDSVACVILTFKEP	248
<i>D. melanogaster</i>	185	QALSDHLAAGLQEDQTYRIDHYLGKEMVQNLMTIRFGNKLSSSTWNRENIASVILTFKEP	244
<i>C. elegans</i>	187	CELSLTHLAKLFKEDQTYRIDHYLGKEMVQNLMLVLRFGNRIILAPSWNRDHIASVILTFKEP	246
p.G248D			
<i>Homo sapiens</i>	241	FGTEGRGGYFDEFGIIRDVMQNHLQLMLCLVAMEKPASTNSDDVRDEKVKVLCISEVQA	300
<i>Mus musculus</i>	241	FGTEGRGGYFDEFGIIRDVMQNHLQLMLCLVAMEKPAATGSSDDVRDEKVKVLCISEVET	300
<i>Danio rerio</i>	249	FGTQGRGGYFDDFGIIRDVMQNHLQLMLSLVAMEKPASTSSDDVRDEKVKVLCIEPVTL	308
<i>D. melanogaster</i>	245	FGTQGRGGYFDEFGIIRDVMQNHLQLMLSLVAMEKPVSCHPDDIRDEKVKVLSIEALT	311
<i>C. elegans</i>	247	FGTGGRGGYFDTAGIIRDVMQNHLMLQILTLVAMEKPAASLNAEDIRDEKVKVLAAKVVEL	306
<i>Homo sapiens</i>	301	NNVVLGQYVGNPDG-EGEATKGYLDDPTVPRGSTTATFAAVVLYVENERWDGVPFILRCGK	360
<i>Mus musculus</i>	301	DNVVLGQYVGNPNPGE-EGEAANGYLDDPTVPHGSTTATFAAAVLYVENERWDGVPFILRCGK	360
<i>Danio rerio</i>	309	SDVVLGQYVGDPDG-EGEAKLGYLDDKTVPKGSTQATFATAVLYVKNRWDGVPFILRCGK	368
<i>D. melanogaster</i>	312	DDMVLGQYLGPNPQGTNDARTGYVEDPTVSNDSTPTYALGVLKINNERWQGVFPFILRCGK	365
<i>C. elegans</i>	307	KDVVVGQYIASPEFDHPEASQGYKDDKSVPADSTPTYALAVVHINNERWEGVFPFILRCGK	367
<i>Homo sapiens</i>	361	ALNERKAEVRLQFHDVAGDIFHQ-QCKRNLVIRVQPNEAVYTKMMTKKPGMFFNPEESEL	420
<i>Mus musculus</i>	361	ALNERKAEVRLQFRDVGADIFHQ-QCKRNLVIRVQPNEAVYTKMMTKKPGMFFNPEESEL	420
<i>Danio rerio</i>	369	ALNERKAEVRLQFTDVPGDIFSS-QCRRNLVIRVQPNEAIVAKMMSKPGVYFSPPEESEL	428
<i>D. melanogaster</i>	366	ALNERKAEVRIQYQDVPGDIFEG-NTKRNLVIRVQPEALYFKMMTKSPGITFDIEESEL	425
<i>C. elegans</i>	368	ALNEKKAERVRIQFKEVSGDIYPSGELKRSSELVMRVQNEAVYMKLMTKPKMGFGVEESEL	428
p.V444I			
<i>Homo sapiens</i>	421	DLTYGNRYKNVKLPDAYERLILDVFCGSQMHFVRSDELREAWRIFTPLHQIELEKPKPI	480
<i>Mus musculus</i>	421	DLTYGNRYKNVKLPDAYERLILDVFCGSQMHFVRSDELREAWRIFTPLHIDREKPPPI	480
<i>Danio rerio</i>	429	DLTYHSRYRDKVLPDAYERLILDVFCGSQMHFVRSDELREAWRIFTPLHQIESEKTPPI	488
<i>D. melanogaster</i>	426	DLTYEHRYKDSYLPDAYERLILDVFCGSQMHFVRSDELREAWRIFTPLHQIEKEHIRPI	485
<i>C. elegans</i>	429	DLTYNNRFKEVRLPDAYERLFLVFMGSQINFVTRDDELEYAWRLITPVLLEELKPKKQPV	488
<i>Homo sapiens</i>	481	PYIYSGRGPTEADELMKRVGFQYEGTYKWNPHKL	515
<i>Mus musculus</i>	481	PVYIYSGRGPTEADELMKRVGFQYEGTYKWNPHKL	515
<i>Danio rerio</i>	489	KYKYSGRGPTEADELVQKGVFRYEGTYKWNPHKL	523
<i>D. melanogaster</i>	486	TYQYSGRGPTEADRKCEENNFKYSGSYKW-----HGGKAATSNH	524
<i>C. elegans</i>	489	QYKFGSRGPTEGDELMKKGYFIFTGTYKVVAP-KL	522

Fig. 2. The similarity alignment of G6PD proteins across different species. The red characters show the corresponding positions of the five substitutions between species whereas the conserved residues were outlined in green box. The species abbreviations are: *D. melanogaster*, *Drosophila melanogaster*; *C. elegans*, *Caenorhabditis elegans*.

Table 2The severity prediction for five newly discovered *G6PD* missense variations.

Nucleotide substitution	Amino acid substitution	SIFT	PolyPhen-2	Mutation Taster	Splicing finder	Conservation ^a	Allele Frequency ^b	Predicted Class ^c
c.187G > A	p.E63K	Tolerated	Benign	Disease causing	Potential alteration	Moderately	<2/1417 ^d	III-IV
c.585G > C	p.Q195H	Damaging	Probably damaging	Disease causing	Potential alteration	Highly	<1/1000	II
c.586A > T	p.I196F	Damaging	Probably damaging	Disease causing	Potential alteration	Highly	<1/1000	II
c.743G > A	p.G248D	Damaging	Probably damaging	Disease causing	Probably no impact	Highly	<1/1000	III
c.1330G > A	p.V444I	Tolerated	Possibly damaging	Disease causing	Potential alteration	Highly	<1/1000	III

^a Sequence comparison between *Homo sapiens*, *Mus musculus*, *Danio rerio* (zebrafish), *Drosophila melanogaster* (fruit fly), and *Caenorhabditis elegans* and *Saccharomyces cerevisiae* as shown in Fig. 2.

^b Allele frequency in Taiwanese population (<https://taiwanview.twbiobank.org.tw/browse38>, accessed on 25 April 2019) [6].

^c Classification of *G6PD* variants in the study according to the WHO definition [7].

^d Two alleles in 1417 people with indeterminate sex.

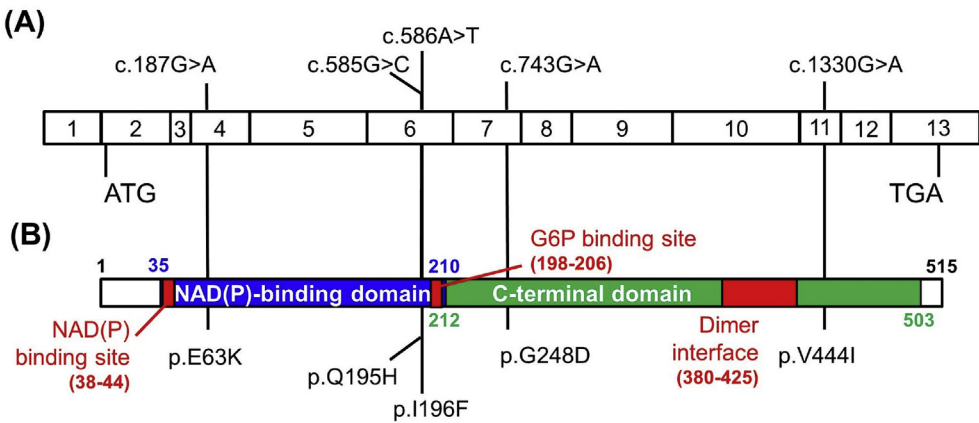


Fig. 3. Schematic representation of alterations in *G6PD* coding regions and protein functional domains. (A) The coding region of the *G6PD* gene containing 13 exons. (B) The *G6PD* protein of 515 amino acids contains two binding domains, namely NAD(P)-binding domain (blue box, amino acids 25–210) and C-terminal domain (green box, amino acids 212–503), and two binding sites, namely NAD(P) binding site (left red box, amino acids 38–44) and G6P-binding site (middle red box, amino acids 198–206), and one dimer interface (right red box, amino acids 380–425). The five mutations were highlighted in black in the coding region and protein domains.

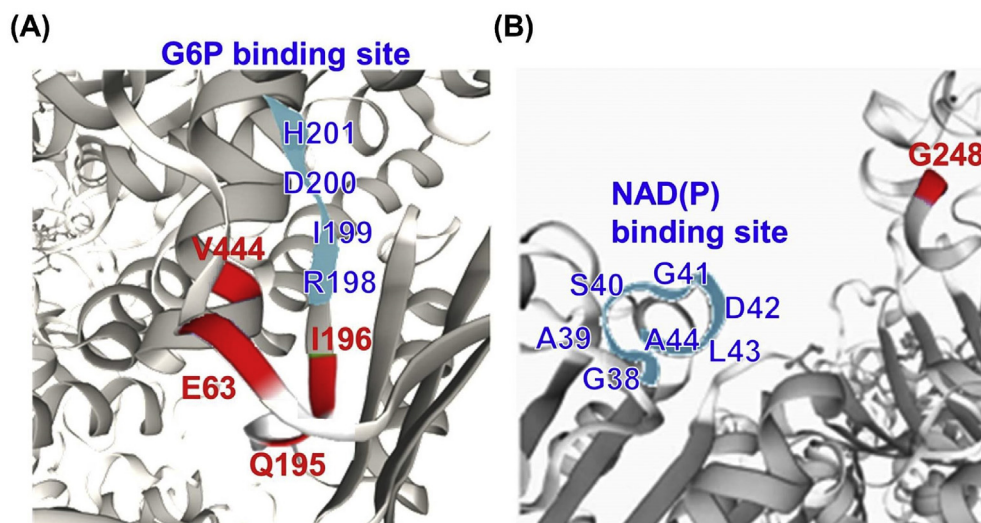


Fig. 4. Close-up views of the ribbon diagram of human G6PD as generated by Swiss PDB viewer. (A) The 3D model structure of G6PD closed to the G6P-binding site, and the Glu63, Gln195, Ile196 and Val444 residuals. (B) A close-up view of G6PD protein contains the NAD(P)-binding site and Gly248 residual. The G6P- and NAD(P)-binding sites were highlighted in cyan, while the residuals were presented in red.

Table 3

Structure prediction of the *G6PD* variations by HOPE algorithm.

Mutants	Structure prediction by HOPE algorithm ^a
p.E63K	The wild-type residue forms a salt bridge with arginine at position 104. The difference in charge will disturb the ionic interaction made by the original, wild-type residue.
p.Q195H	The wild-type residue forms a hydrogen bond with arginine at position 192. The size difference between wild-type and mutant residue makes that the new residue is not in the correct position to make the same hydrogen bond as the original wild-type residue did.
p.I196F	The mutant residue is bigger than the wild-type residue and is located in a domain that is important for the activity of the protein and in contact with residues in another domain. The mutation can affect this interaction and as such affect protein function.
p.G248D	The wild-type residue is a glycine, the most flexible of all residues. This flexibility might be necessary for the protein's function. Mutation of this glycine can abolish this function.
p.V444I	The mutant residue is bigger than the wild-type residue and is located in a domain that is important for binding of other molecules. The mutation might affect this interaction and thereby disturb signal transfer from binding domain to the activity domain.

^a Using software Have yOur Protein Explained (HOPE, <http://www.cmbi.ru.nl/hope/>) [9].

Acknowledgments

This research was supported by the Taipei City Government, Taiwan [grant number 10501-62-058], and Taipei City Hospital, Taiwan [grant number TPCH-103-002].

Conflict of Interest

The authors declare that they have no known competing financial interests or personal relationships that could have appeared to influence the work reported in this paper.

References

- [1] Y.H. Chiu, H.J. Chen, Y.C. Chang, Y.N. Liu, S.M. Kao, M.Y. Liu, et al., Applying a multiplexed primer extension method on dried blood spots increased the detection of carriers at risk of glucose-6-phosphate dehydrogenase deficiency in newborn screening program, *Clin. Chim. Acta* 495 (2019) 271–277. <https://doi.org/10.1016/j.cca.2019.04.074>.
- [2] M.A. Larkin, G. Blackshields, N.P. Brown, R. Chenna, P.A. McGettigan, H. McWilliam, et al., Clustal W and clustal X version 2.0, *Bioinformatics* 23 (2007) 2947–2948.
- [3] S.E. Flanagan, A.M. Patch, S. Ellard, Using SIFT and PolyPhen to predict loss-of-function and gain-of-function mutations, *Genet. Test. Mol. Biomark.* 14 (2010) 533–537. <https://doi:10.1089/gtmb.2010.0036>.
- [4] J.M. Schwarz, D.N. Cooper, M. Schuelke, D. Seelow, MutationTaster2: mutation prediction for the deep-sequencing age, *Nat. Methods* 11 (2014) 361–362. <https://doi:10.1038/nmeth.2890>.
- [5] F.O. Desmet, D. Hamroun, M. Lalonde, G. Collod-Bérout, M. Claustres, C. Bérout, Human Splicing Finder: an online bioinformatics tool to predict splicing signals, *Nucleic Acids Res.* 37 (2009) e67. <https://doi:10.1093/nar/gkp215>.
- [6] Taiwan Biobank, Genetic and Medical Information for Taiwan, 2019 accessed, <https://taiwanview.twbiobank.org.tw/browse38>. (Accessed 25 April 2019).
- [7] M.D. Cappellini, G. Fiorelli, Glucose-6-phosphate dehydrogenase deficiency, *Lancet* 37 (2008) 64–74. [https://doi:10.1016/S0140-6736\(08\)60073-2](https://doi:10.1016/S0140-6736(08)60073-2).
- [8] S.W. Au, S. Gover, V.M. Lam, M.J. Adams, Human glucose-6-phosphate dehydrogenase: the crystal structure reveals a structural NADP(+) molecule and provides insights into enzyme deficiency, *Structure* 8 (2000) 293–303.
- [9] H. Venselaar, T.A. Te Beek, R.K. Kuipers, M.L. Hekkelman, G. Vriend, Protein structure analysis of mutations causing inheritable diseases. An e-Science approach with life scientist friendly interfaces, *BMC Bioinf.* 11 (2010) 548. <https://doi:10.1186/1471-2105-11-548>.
- [10] S.H. Chiang, M.L. Fan, K.J. Hsiao, External quality assurance programme for newborn screening of glucose-6-phosphate dehydrogenase deficiency, *Ann. Acad. Med. Singapore* 37 (2008) 84.
- [11] J.R.C. Muniz, N.W. Szeto, R. Frise, W.H. Lee, X.S. Wang, B. Thöny, et al., Role of protein structure in variant annotation: structural insight of mutations causing 6-pyruvoyl-tetrahydropterin synthase deficiency, *Pathology* 51 (2019) 274–280. <https://doi:10.1016/j.pathol.2018.11.011>.